

Enhanced Superconductivity and Suppression of Charge-density Wave Order in 2H-TaS₂ in the Two-dimensional Limit

Yafang Yang,¹ Shiang Fang,² Valla Fatemi,¹ Jonathan Ruhman,¹ Efrén Navarro-Moratalla,³ Kenji Watanabe,⁴ Takashi Taniguchi,⁴ Efthimios Kaxiras,^{2,5} and Pablo Jarillo-Herrero^{1,*}

¹*Department of Physics, Massachusetts Institute of Technology, Cambridge, MA 02139 USA*

²*Department of Physics, Harvard University, Cambridge, Massachusetts 02138, USA*

³*Instituto de Ciencia Molecular, Universidad de Valencia, c/Catedrático José Beltrán 2, 46980 Paterna, Spain*

⁴*National Institute for Materials Science, Namiki 1-1, Tsukuba, Ibaraki 305-0044, Japan*

⁵*John A. Paulson School of Engineering and Applied Sciences, Harvard University, Cambridge, Massachusetts 02138, USA*

(Dated: December 14, 2024)

As superconductors are thinned down to the 2D limit, their critical temperature T_c typically decreases. Here we report the opposite behavior, an enhancement of T_c with decreasing thickness, in the 2D crystalline superconductor 2H-TaS₂. Remarkably, in the monolayer limit, T_c increases by over a factor of four compared to bulk crystals. Accompanying this trend in superconductivity, we observe progressive weakening and suppression of the charge-density wave (CDW) transition with decreasing thickness. To explain these trends, we perform electronic structure calculations showing that a reduction of the CDW amplitude results in a substantial increase of the density of states at the Fermi energy, which contributes to the enhancement of T_c . Our results establish ultra-thin 2H-TaS₂ as an ideal platform to study the competition between CDW order and superconductivity.

Transition metal dichalcogenides (TMDs) 2H-MX₂ (where M = Nb, Ta and X = S, Se) have attracted considerable attention as intriguing 2D crystalline superconductors [1]. In these materials, superconductivity (SC) forms in an environment of pre-existing charge-density wave (CDW) order [2, 3], making it an ideal platform to study many-body ground states and competing phases in the 2D limit. In bulk crystals, the reported critical temperature of the CDW transition decreases from 120 K in 2H-TaSe₂ down to 30 K in 2H-NbSe₂. Superconductivity weakens in approximately reverse order, with T_c increasing from around 0.2 K in 2H-TaSe₂ to 7.2 K in 2H-NbSe₂. The relationship between CDW and superconductivity in such systems is still under debate [4, 5]. It is generally believed that such mutual interaction is competitive, but evidence to the contrary, indicating a cooperative interaction, has also been reported in angular-resolved photoemission spectroscopy studies [3].

In TMDs, superconductivity and CDW instability can be investigated by adjusting the interlayer interactions through pressure [6, 7] or molecule intercalation [8, 9]. Recently, mechanical exfoliation has emerged as a robust method for producing ultra-clean, highly crystalline samples with atomic thickness [10]. This offers a useful way to assess the effect of dimensionality and interlayer interactions on superconductivity and CDW. A material whose behavior as a function of layer thickness has been recently studied is 2H-NbSe₂ [11–13], in which the superconducting state is progressively weaker in thinner samples, with T_c reduced from 7 K in bulk crystals to 3 K in the monolayer. This monotonic decrease of superconducting T_c can be attributed to a weaker interlayer Cooper pairing as thickness is reduced [12]. The

thickness dependence of CDW order is still under debate, considering discrepancies between Raman and scanning tunneling microscopy/spectroscopy (STM/STS) studies [14, 15].

Bulk 2H-TaS₂, another member of the 2H-MX₂ family, exhibits a CDW transition at 70 K and a SC transition at 0.8 K [2, 16–18]. Compared to 2H-NbSe₂, 2H-TaS₂ manifests a stronger signature of CDW transition in transport in the form of a sharp decrease of resistivity [9], and thus serves as a desirable platform to study the thickness dependence of CDW instability and superconductivity. A prior study observed an enhanced T_c down to thickness of 3.5 nm, utilizing 2H-TaS₂ flakes directly exfoliated on a Si/SiO₂ substrate [18]. Unfortunately, it was found that samples thinner than that become insulating, indicative of its particular susceptibility to degradation in ambient atmosphere. Therefore, exfoliation and encapsulation in an inert atmosphere become crucial to attain high quality samples. Here we report that superconductivity persists in 2H-TaS₂ down to the single-layer limit, with a pronounced increase in T_c from 0.8 K in bulk crystals to 3.4 K in the monolayer. A careful investigation on $R(T)$ behavior at higher temperatures reveals a suppression of the CDW order as thickness is decreased. In search of an origin of such trends, we perform electronic structure calculations and investigate the change in the band structure and density of states (DOS) at the Fermi level $N(E_F)$ as a function of CDW amplitude. We show that suppression of the CDW order leads to a substantial increase in $N(E_F)$, which ultimately enhances T_c . Our observation also motivates consideration of quantum fluctuations of the CDW order as another mechanism that boosts T_c . This provides new insights into the impact

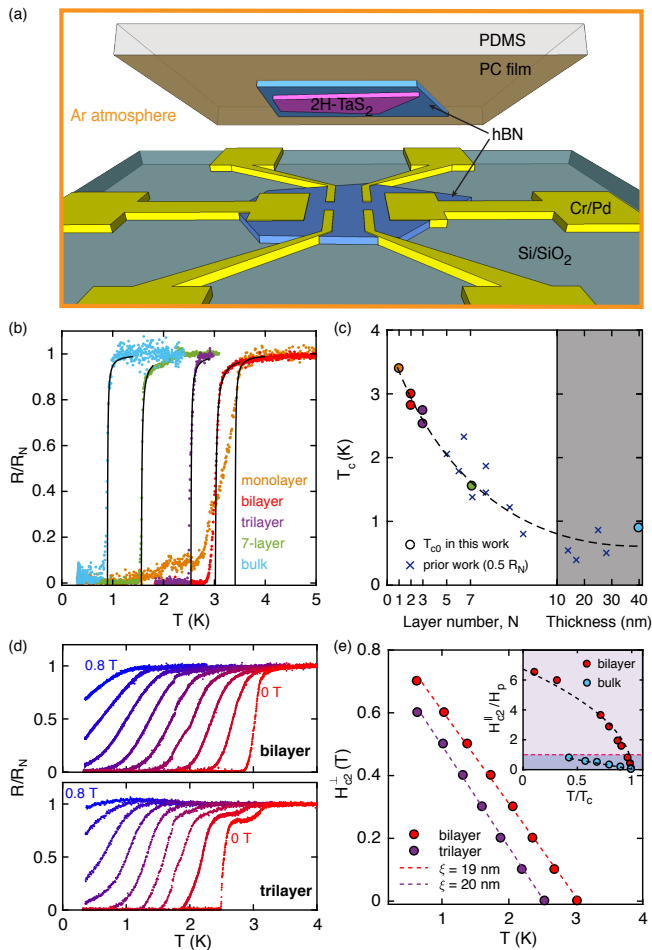


FIG. 1. (a) Schematic of device fabrication. (b) Resistance normalized by the normal state (R/R_N) as a function of temperature for monolayer, bilayer, trilayer, 7-layer and bulk samples near the SC transition. The superconducting T_c is 3.4, 3.0, 2.5, 1.6 and 0.9 K respectively, determined by fitting the transition curve to the Aslamazov-Larkin formula (black solid lines). (c) T_c reported in this work (circles) and in a prior study (crosses) [18]. The dashed line guides the eye to the general trend. (d) Top (bottom) panel: Temperature dependent resistance of bilayer (trilayer) under out-of-plane magnetic fields (0, 0.1, ..., 0.8 T). (e) Out-of-plane critical field H_{c2}^{\perp} for bilayer and trilayer samples. The dashed lines are linear fits to $H_{c2}^{\perp} = \phi_0/(2\pi\xi(0)^2)(1 - T/T_c)$, where ϕ_0 , $\xi(0)$ denote the flux quantum and in-plane GL coherence length at zero temperature respectively. Inset: In-plane critical field H_{c2}^{\parallel} normalized by Pauli limit ($H_p \approx 1.86T_c$) for bilayer and bulk samples. The dashed line for bilayer is a fit to the Tinkham formula for 2D samples $H_{c2}^{\parallel} = \sqrt{12}\phi_0/(2\pi\xi(0)d)\sqrt{(1 - T/T_c)}$ [19]. The purple background indicates the Pauli limit regime.

of reduced dimensions on many-body ground states and their interactions.

In this work, we exfoliate and fabricate samples with a transfer set-up built inside a glove box filled with Argon gas, and encapsulate the TaS₂ flake between two sheets of hexagonal boron nitride. We build our devices utilizing

a polymer pick-up technique [20] as illustrated in Fig. 1 (a), taking advantage of the van der Waals adhesion between 2D layers (see Supplemental Material [21]). With this method, we are able to obtain high quality few-layer 2H-TaS₂ devices. As seen in Fig. 1 (b), when temperature is sufficiently low, a clear superconducting transition is observed for monolayer, bilayer, trilayer, 7-layer, and bulk (thickness ~ 40 nm) samples. By fitting the resistance to the Aslamazov-Larkin expression [22], we are able to determine the mean-field superconducting transition temperature T_c . When sample thickness is decreased from bulk to monolayer, the corresponding T_c monotonically increases from 0.9 K to 3.4 K [23]. The trend observed in our experiment is strictly opposite that of a previous finding on 2H-NbSe₂ [12], where T_c decreases monotonically with thickness reduction, despite the fact that the two materials are isostructural and isovalent. In 2H-NbSe₂, the decreased T_c is attributed to a weaker interlayer Cooper pairing given by $\lambda_{inter} \sim \cos(\pi/(N+1))$ as layer number N is reduced. In our case, however, it is surprising to see that even with a reduced interlayer Cooper pairing, the T_c can be dramatically enhanced by more than a factor of four. To verify the validity of the thickness dependence of T_c in a wider range of thicknesses and against varying extrinsic parameters (level of disorder, substrate, source of crystal, sample quality etc.), we measure an additional set of bilayer and trilayer samples and plot our results alongside previously reported T_c values [18] in Fig. 1 (c). Regardless of different sample preparation procedures and substrates, the trend of T_c versus thickness is consistent between the two sets of experimental results, indicative of an intrinsic origin underlying the enhancement of T_c .

To further characterize the superconducting properties of thin 2H-TaS₂, we study the superconducting transition under both out-of-plane and in-plane magnetic fields. Fig. 1 (d) shows the temperature dependence of the normalized resistance (R/R_N) for bilayer and trilayer samples at various out-of-plane magnetic fields. The H_{c2}^{\perp} is thus extracted as a function of temperature, shown in Fig. 1 (e). Close to T_c , the dependence of H_{c2}^{\perp} is fitted well by the phenomenological 2D Ginzburg-Landau (GL) model, which yields $\xi(0) = 19$ nm (bilayer) and $\xi(0) = 20$ nm (trilayer), where $\xi(0)$ denotes the GL coherence length at zero temperature. For in-plane field, we observe a much larger $H_{c2}^{\parallel} = 32$ T at 300 mK for a bilayer ($T_c = 2.8$ K), which is more than six times the Pauli paramagnetic limit H_p , obeying a square root rather than a linear temperature dependence (inset of Fig. 1 (e)). This dramatic enhancement of in-plane H_{c2}^{\parallel} , often referred to as Ising superconductivity, has been observed in other 2D crystalline superconductors [12, 13, 24, 25].

The above observation verifies that atomically thin 2H-TaS₂ behaves as a 2D superconductor. In the Supplemental Material [21], we also show that the superconduct-

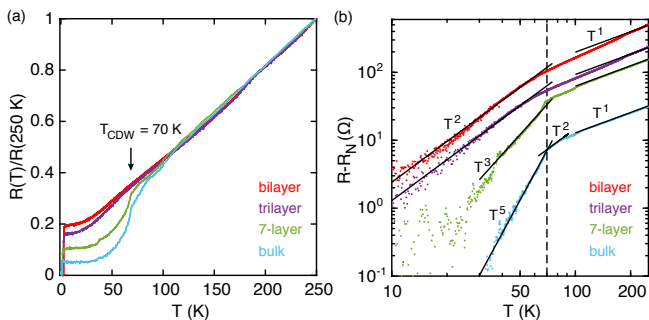


FIG. 2. (a) Normalized resistance $R(T)/R(250\text{K})$ for bilayer, trilayer, 7-layer and bulk samples, measured during cooling down. T_{CDW} is characterized by a sharp kink in the resistance. (b) Resistance $R - R_N$ vs. T plotted in a log-log scale, where R_N is the residual resistance above the onset temperature of superconductivity.

ing transition also exhibits the Berezinskii-Kosterlitz-Thouless (BKT) transition as expected in 2D. However, it remains unclear what mechanism drives T_c to be nearly four-fold larger in the monolayer than that in bulk crystals. To gain better understanding of the thickness dependent behavior of this material, we characterize the normal state resistance of 2H-TaS₂ in the same samples as a function of temperature. Shown in Fig. 2 (a) is a plot of normalized resistance versus temperature on a linear scale. All samples manifest a linear decrease of resistance at high temperatures, consistent with phonon limited resistivity in a normal metal [26]. Below 70 K, the 7-layer and bulk devices undergo a sudden drop in resistance, indicating the CDW transition. In bilayer and trilayer, however, such drop is not noticeable. The anomalous drop of resistivity observed in thicker samples can be understood by the Rice-Scott ‘saddle point’ mechanism [27]. As we show in the Supplemental Material [21], the Fermi surface of 2H-TaS₂ comprises two double-wall hole pockets around Γ and K. An extended saddle band very close to E_F connects these pockets along Γ -K, producing van Hove singularities. The saddle points act as scattering ‘sinks’, and their removal by the CDW order suppresses the dc resistivity.

In order to appreciate in detail the temperature dependence of the sample resistivity, we plot the subtracted resistance $R - R_N$ of the same four devices on a log-log scale in Fig. 2 (b). The result is remarkable: for bulk and 7-layer, the linear temperature dependence is disrupted by a sudden switch to T^5 and T^3 near T_{CDW} . In contrast, a gradual transition from linear to T^2 is observed in bi-/tri-layer, showing no evidence of abrupt transition. The three distinctive low-T power-law behaviors, which reflect different underlying carrier scattering mechanisms, can be interpreted as a result of progressive weakening of the CDW order.

In solids, $\rho \sim T^5$ has been well understood as a consequence of electron-phonon scattering at temperatures

lower than the Debye temperature Θ_D . Prior experiment shows that the temperature dependence of resistivity switches from $\rho \sim T^5$ in Ta dichalcogenides to $\rho \sim T^3$ in Nb dichalcogenides [28], for which the CDW transition has much weaker impact on DOS at the Fermi level [29]. It has been pointed out that a weaker CDW order will result in higher $N(E_F)$, and consequently, an increased rate of interband scattering, leading to a predominant T^3 behavior in Nb dichalcogenides. We speculate that the crossover from T^5 to T^3 observed in our samples is due to the same origin. In contrast, bi-/tri-layer manifests a quadratic behavior at low temperatures. This seems to agree well with Fermi liquid theory on electron-electron (e-e) scattering. However, assuming e-e scattering is not greatly altered from 3D to 2D (for detailed calculations, see Supplemental Material [21]), it is implausible that the T^2 behavior is completely absent in thick samples in the same temperature range. Here we propose another possible mechanism that leads to a T^2 resistivity: scattering of electrons by soft phonons, i.e. critical CDW fluctuations, which can happen close to a finite momentum ordering transition [30] (see Supplemental Material [21]). Therefore the T^2 behavior in ultra-thin samples can be interpreted as indications of existence of soft phonons, which forms in the proximity to a CDW transition. Additionally, this can also explain the T^2 behavior observed in the bulk sample at temperatures above the CDW transition. The stunning difference of $R(T)$ behavior manifested in different thicknesses reveals the rich physics embodied in transport measurement of 2H-TaS₂.

It is worth noting that a similar anti-correlation of trends of SC and CDW transition has also been observed in 2H-TaS₂ crystals under pressure [6] and single crystal alloys [31–33]. To better understand the connection between CDW and superconductivity, we recall that in McMillan’s theory, the critical temperature is expressed as [34]

$$T_c = \frac{\Theta_D}{1.45} \exp\left[-\frac{1.04(1+\lambda)}{\lambda - \mu^*(1+0.62\lambda)}\right], \quad (1)$$

where μ^* is the Coulomb pseudopotential of Morel and Anderson

$$\mu^* = \frac{N(E_F)\langle V_c \rangle}{1 + N(E_F)\langle V_c \rangle \ln\left(\frac{E_B}{\omega_0}\right)}, \quad (2)$$

and λ is the electron-phonon coupling constant

$$\lambda = N(E_F)\langle I^2 \rangle / M\langle \omega^2 \rangle. \quad (3)$$

Here $N(E_F)$ is the band structure density of states, V_c is the matrix element of the screened Coulomb interaction, E_B is the electronic band width, ω (ω_0) is the (maximum) phonon frequency, I is the electron-phonon matrix elements, M is the atom mass, and $\langle \dots \rangle$ is the average over the Fermi surface. In the weak-coupling regime ($\lambda \ll 1$), Eq. (1) reduces to the Bardeen-Cooper-Schrieffer (BCS)

result with $\lambda - \mu^*$ playing the role of $N(E_F)V$. Assuming $\mu^* = 0.15$ as suggested by McMillan [34], one can evaluate the inverted form of Eq. (1) and obtain $\lambda = 0.482$ for 2H-TaS₂ with $\Theta_D = 250$ K [35] and $T_c = 0.8$ K [18], indicating that 2H-TaS₂ lies in the intermediate coupling regime.

The CDW instability allows electronic systems to lower their energy by inducing energy gaps in the spectrum. Since $N(E_F)$ plays an important role in determining T_c , here we perform electronic structure calculations based on density functional theory (DFT), as implemented in VASP code [36, 37] in order to obtain the DOS in the normal and the CDW phases. We focus our study on three representative thicknesses: monolayer, bilayer and bulk, and the main results are summarized in Fig. 3 (b), (c). A comparison of Fig. 3 (b) and (c) reveals an appreciable reduction of DOS near the Fermi level induced by CDW order for all three thicknesses. This is consistent with previous magnetic susceptibility and heat capacity experiments showing a sharp drop of density of states below the CDW transition [38, 39]. Further, to visualize the effects of CDW on the pristine band structure, we derive the unfolded band structure in the CDW phase, shown in Fig. 3 (a), based on the Fourier decompositions of the Bloch wavefunctions from the tight-binding Hamiltonians [40, 41] (see Supplemental Material [21]). It is clearly seen that a band gap, Δ_{CDW} , emerges in the inner pocket around K along Γ -K and K-M. In addition, the saddle point located along the Γ -K, is shifted to energies above the Fermi level, in agreement with the Rice-Scott model. These explain the substantial decrease of $N(E_F)$ induced by the CDW order.

We investigate the progressive weakening of CDW with decreasing thickness by varying the magnitude of atomic distortion. A scaling factor, from 1 to 0, is used to define the fraction by which the magnitude of the atomic displacement is reduced with respect to the stable distorted configuration. The corresponding DOS as a function of the CDW amplitude is calculated and plotted in Fig. 3 (d). Using $\lambda_{bulk} = 0.482$, $\mu^* = 0.15$, $N(E_F) = 1.78$ states/eV/f.u. (f.u. stands for formula unit) for bulk as a starting point, we calculate λ and μ^* , and ultimately T_c , as a function of $N(E_F)$ within the McMillan formalism, assuming no other parameters change. The prediction of T_c is plotted in Fig. 3 (e). It is remarkable that an enhancement of T_c up to 3.4 K is reproduced when the amplitude of CDW goes to zero. This result provides evidence for the competitive nature of the interaction between CDW order and SC. We note that our analysis is simplified to exclude variation of parameters such as Θ_D , electron-phonon matrix element and the phonon spectrum.

This is not the first experiment indicating that a CDW phase transition vanishes in reduced dimensions [8, 42–45]. One explanation is associated with reduced interlayer interaction due to the intercalation/exfoliation pro-

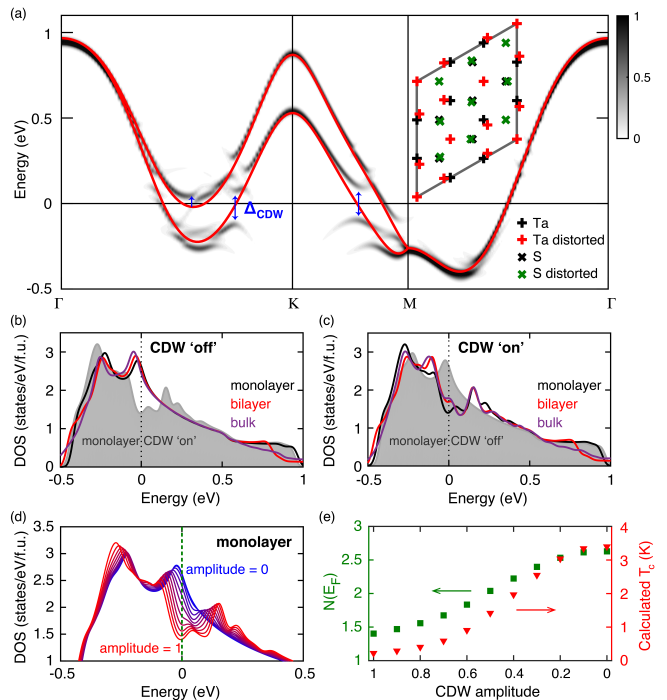


FIG. 3. (a) Band structure for monolayer 2H-TaS₂. The grey lines show the unfolded band structure compared with original band structure in the normal phase (red lines). Inset illustrates the position and displacement of Ta/S atoms before and after CDW transition in real space. (b) Density of states for monolayer/bilayer/bulk in the normal phase. Monolayer in the CDW phase is plotted as a grey shade for reference. (c) Density of states for monolayer/bilayer/bulk in the CDW phase. Monolayer in the normal phase is plotted as a grey shade for reference. (d) A comparison of density of states close to Fermi level for monolayer with various CDW amplitudes ranging from 1 (full amplitude) to 0 (total suppression). (e) Left axis: density of states at Fermi level $N(E_F)$ as a function of CDW amplitude for monolayer. Right axis: T_c from Eq. (1) using calculated $N(E_F)$.

cess [42]. Nevertheless, DFT calculations suggest that the CDW instability remains robust upon removal of the interlayer interactions [5]. Recently, a study showed that lattice fluctuations arising from the strong electron-phonon coupling act to suppress the onset temperature of CDW order, leading to a pseudogap phase characterized by local order and strong phase fluctuations [46]. This is consistent with our model of presence of soft phonons, or CDW fluctuations [28] as primary contributor to the T^2 behavior of resistivity observed above T_{CDW} . More interestingly, theory predicts that quantum fluctuations caused by proximity to a CDW transition can boost superconducting pairing by providing sources of bosonic excitations [47]. Although there is no direct evidence that CDW fluctuations facilitate superconductivity in 2H-TaS₂, this scenario reveals a potentially rich relationship between CDW and SC.

In conclusion, we observe enhanced superconductivity

in atomically thin 2H-TaS₂ accompanied with suppression of the CDW order. Our electronic band structure calculation shows that suppression of the CDW phase leads to a substantial increase in $N(E_F)$, which acts to boost the superconducting T_c . We further suggest that the emergence of $R \sim T^2$ behavior in ultra-thin samples is attributable to the scattering of electrons with soft phonon modes, indicative of critical CDW fluctuations. Systematic studies of the layer dependence of the CDW order, for example, STM/STS and ultrafast spectroscopy studies, will be essential to understanding both the origin of the CDW and the relationship between CDW and superconductivity.

We thank Yuan Cao and Jason Luo for experimental help. We also thank Patrick A. Lee, Dennis Huang, Miguel A. Cazalilla and Bertrand I. Halperin for fruitful discussions. This work has been primarily supported by the US DOE, BES Office, Division of Materials Sciences and Engineering under Award DE-SC0001819 (YY and PJH) and by the Gordon and Betty Moore Foundations EPiQS Initiative through Grant GBMF4541 to PJH. Fabrication work (ENM) and theory analysis were partly supported by the NSF-STC Center for Integrated Quantum Materials under award No. DMR-1231319 (VF, SF) and ARO MURI Award W911NF-14-0247 (EK). This work made use of the MRSEC Shared Experimental Facilities supported by NSF under award No. DMR-0819762 and of Harvards CNS, supported by NSF under Grant ECS-0335765. SF used Odyssey cluster of the FAS by the Research Computing Group at Harvard University, and the Extreme Science and Engineering Discovery Environment, which is supported by NSF Grant No. ACI-1053575. JR acknowledges the Gordon and Betty Moore Foundation under the EPiQS initiative under Grant No. GBMF4303. A portion of this work was performed at the National High Magnetic Field Laboratory, which is supported by NSF Cooperative Agreement No. DMR-1157490 and the State of Florida. Growth of hexagonal boron nitride crystals was supported by the Elemental Strategy Initiative conducted by the MEXT, Japan and JSPS KAKENHI Grant Numbers JP15K21722 and JP25106006.

* pjarillo@mit.edu

- [1] Y. Saito, T. Nojima, and Y. Iwasa, *Nat. Rev. Mater.* **2** (2016).
- [2] A. C. Neto, *Phys. Rev. Lett.* **86**, 4382 (2001).
- [3] T. Kiss, T. Yokoya, A. Chainani, S. Shin, T. Hanaguri, M. Nohara, and H. Takagi, *Nat. Phys.* **3**, 720 (2007).
- [4] M. Calandra, I. Mazin, and F. Mauri, *Phys. Rev. B* **80**, 241108 (2009).
- [5] Y. Ge and A. Y. Liu, *Phys. Rev. B* **86**, 104101 (2012).
- [6] D. Freitas, P. Rodiere, M. Osorio, E. Navarro-Moratalla, N. Nemes, V. Tissen, L. Cario, E. Coronado, M. García-Hernández, S. Vieira, *et al.*, *Phys. Rev. B* **93**, 184512 (2016).
- [7] C. Chu, V. Diatschenko, C. Huang, and F. DiSalvo, *Phys. Rev. B* **15**, 1340 (1977).
- [8] A. Thompson, F. Gamble, and R. Koehler Jr, *Phys. Rev. B* **5**, 2811 (1972).
- [9] J. A. Wilson, F. Di Salvo, and S. Mahajan, *Adv. in Phys.* **24**, 117 (1975).
- [10] A. K. Geim and K. S. Novoselov, *Nat. Mater.* **6**, 183 (2007).
- [11] Y. Cao, A. Mishchenko, G. Yu, E. Khestanova, A. Rooney, E. Prestat, A. Kretinin, P. Blake, M. Shalom, C. Woods, *et al.*, *Nano Lett.* **15**, 4914 (2015).
- [12] X. Xi, Z. Wang, W. Zhao, J.-H. Park, K. T. Law, H. Berger, L. Forró, J. Shan, and K. F. Mak, *Nat. Phys.* **12**, 139 (2016).
- [13] A. W. Tsen, B. Hunt, Y. D. Kim, Z. J. Yuan, S. Jia, R. J. Cava, J. Hone, P. Kim, C. R. Dean, and A. N. Pasupathy, *Nat. Phys.* **12**, 208 (2016).
- [14] X. Xi, L. Zhao, Z. Wang, H. Berger, L. Forró, J. Shan, and K. F. Mak, *Nat. Nanotechnol.* **10**, 765 (2015).
- [15] M. M. Ugeda, A. J. Bradley, Y. Zhang, S. Onishi, and Y. Chen, *Nat. Phys.* **12**, 92 (2015).
- [16] S. Nagata, T. Aochi, T. Abe, S. Ebisu, T. Hagino, Y. Seki, and K. Tsutsumi, *J. Phys. Chem. Solids* **53**, 1259 (1992).
- [17] I. Guillamón, H. Suderow, J. G. Rodrigo, S. Vieira, P. Rodière, L. Cario, E. Navarro-Moratalla, C. Martí-Gastaldo, and E. Coronado, *New J. Phys.* **13**, 103020 (2011).
- [18] E. Navarro-Moratalla, J. O. Island, S. Mañas-Valero, E. Pinilla-Cienfuegos, A. Castellanos-Gomez, J. Queda, G. Rubio-Bollinger, L. Chirolli, J. A. Silva-Guillén, N. Agrait, G. A. Steele, F. Guinea, H. S. J. van der Zant, and E. Coronado, *Nat. Commun.* **7**, 11043 (2016).
- [19] M. Tinkham, *Introduction to superconductivity* (Dover, New York, 2004).
- [20] J. I.-J. Wang, Y. Yang, Y.-A. Chen, K. Watanabe, T. Taniguchi, H. O. Churchill, and P. Jarillo-Herrero, *Nano Lett.* **15**, 1898 (2015).
- [21] See Supplemental Material for further details.
- [22] L. Aslamasov and A. Larkin, *Phys. Lett. A* **26**, 238 (1968).
- [23] For the monolayer flake, determination of T_c becomes tricky due to electrical shortage to adjacent flakes with different thickness. Detailed analysis and determination of T_c by critical current mapping can be found in Supplemental Material [21].
- [24] J. Lu, O. Zheliuk, I. Leermakers, N. F. Yuan, U. Zeitler, K. T. Law, and J. Ye, *Science* **350**, 1353 (2015).
- [25] Y. Saito, Y. Nakamura, M. S. Bahramy, Y. Kohama, J. Ye, Y. Kasahara, Y. Nakagawa, M. Onga, M. Tokunaga, T. Nojima, *et al.*, *Nat. Phys.* **12**, 144 (2016).
- [26] M. S. El-Bana, D. Wolverson, S. Russo, G. Balakrishnan, D. M. Paul, and S. J. Bending, *Supercond. Sci. Technol.* **26**, 125020 (2013).
- [27] T. Rice and G. Scott, *Phys. Rev. Lett.* **35**, 120 (1975).
- [28] M. Naito and S. Tanaka, *J. Phys. Soc. Jpn.* **51**, 219 (1982).
- [29] M. Marezio, P. Dernier, A. Menth, and G. Hull, *J. Solid State Chem.* **4**, 425 (1972).
- [30] R. Hlubina and T. Rice, *Phys. Rev. B* **51**, 9253 (1995).

- [31] K. E. Wagner, E. Morosan, Y. S. Hor, J. Tao, Y. Zhu, T. Sanders, T. M. McQueen, H. W. Zandbergen, A. J. Williams, D. V. West, and R. J. Cava, *Phys. Rev. B* **78**, 104520 (2008).
- [32] L. Fang, P. Y. Zou, Y. Wang, L. Tang, Z. Xu, H. Chen, C. Dong, L. Shan, and H. H. Wen, *Sci. Technol. Adv. Mater.* **6**, 736 (2016).
- [33] L. Li, X. Deng, Z. Wang, Y. Liu, and M. Abeykoon, *npj Quant. Mater.* **2**, 11 (2017).
- [34] W. McMillan, *Phys. Rev.* **167**, 331 (1968).
- [35] A. Schlicht, M. Schwenker, W. Biberacher, and A. Lerf, *J. Phys. Chem. B* **105**, 4867 (2001).
- [36] G. Kresse and J. Furthmüller, *Phys. Rev. B* **54**, 11169 (1996).
- [37] G. Kresse and J. Furthmüller, *Comput. Mater. Sci.* **6**, 15 (1996).
- [38] F. Di Salvo, R. Schwall, T. Geballe, F. Gamble, and J. Osiecki, *Phys. Rev. Lett.* **27**, 310 (1971).
- [39] L. Mattheiss, *Phys. Rev. B* **8**, 3719 (1973).
- [40] M. Farjam, arXiv:1504.04937 (2015).
- [41] V. Popescu and A. Zunger, *Phys. Rev. B* **85**, 085201 (2012).
- [42] A. Ayari, E. Cobas, O. Ogundadegbe, and M. S. Fuhrer, *J. Appl. Phys.* **101**, 014507 (2007).
- [43] J. Pan, C. Guo, C. Song, X. Lai, H. Li, W. Zhao, H. Zhang, G. Mu, K. Bu, T. Lin, X. Xie, M. Chen, and F. Huang, *J. Am. Chem. Soc.* **139**, 4623 (2017).
- [44] C. E. Sanders, M. Dendzik, A. S. Ngankeu, A. Eich, A. Bruix, M. Bianchi, J. A. Miwa, B. Hammer, A. A. Khajetoorians, and P. Hofmann, *Phys. Rev. B* **94**, 081404 (2016).
- [45] M. Yoshida, R. Suzuki, Y. Zhang, M. Nakano, and Y. Iwasa, *Sci. Adv.* **1**, e1500606 (2015).
- [46] F. Flicker and J. van Wezel, *Phys. Rev. B* **94**, 235135 (2016).
- [47] Y. Wang and A. V. Chubukov, *Phys. Rev. B* **92**, 125108 (2015).